Atmos. Meas. Tech., 8, 1555–1573, 2015
www.atmos-meas-tech.net/8/1555/2015/
doi:10.5194/amt-8-1555-2015

Atmospheric Measurement Techniques
Open Access

Using XCO_2 retrievals for assessing the long-term consistency of NDACC/FTIR data sets

S. Barthlott[1], M. Schneider[1], F. Hase[1], A. Wiegele[1], E. Christner[1], Y. González[2], T. Blumenstock[1], S. Dohe[1], O. E. García[2], E. Sepúlveda[2], K. Strong[3], J. Mendonca[3], D. Weaver[3], M. Palm[4], N. M. Deutscher[4,6], T. Warneke[4], J. Notholt[4], B. Lejeune[5], E. Mahieu[5], N. Jones[6], D. W. T. Griffith[6], V. A. Velazco[6], D. Smale[7], J. Robinson[7], R. Kivi[8], P. Heikkinen[8], and U. Raffalski[9]

[1]Institute for Meteorology and Climate Research (IMK-ASF), Karlsruhe Institute of Technology (KIT), Karlsruhe, Germany
[2]Izaña Atmospheric Research Center, Agencia Estatal de Meteorología (AEMET), Tenerife, Spain
[3]Department of Physics, University of Toronto (UofT), Toronto, Canada
[4]Institute of Environmental Physics, University of Bremen (UB), Bremen, Germany
[5]Institute of Astrophysics and Geophysics, University of Liège (ULG), Liège, Belgium
[6]Centre for Atmospheric Chemistry, University of Wollongong (UOW), Wollongong, Australia
[7]National Institute of Water and Atmospheric Research (NIWA), Lauder, New Zealand
[8]Arctic Research, Finnish Meteorological Institute (FMI), Helsinki, Finland
[9]The Swedish Institute of Space Physics (IRF), Kiruna, Sweden

Correspondence to: S. Barthlott (sabine.barthlott@kit.edu)

Received: 6 August 2014 – Published in Atmos. Meas. Tech. Discuss.: 16 October 2014
Revised: 5 February 2015 – Accepted: 21 February 2015 – Published: 25 March 2015

Abstract. Within the NDACC (Network for the Detection of Atmospheric Composition Change), more than 20 FTIR (Fourier-transform infrared) spectrometers, spread worldwide, provide long-term data records of many atmospheric trace gases. We present a method that uses measured and modelled XCO_2 for assessing the consistency of these NDACC data records. Our XCO_2 retrieval setup is kept simple so that it can easily be adopted for any NDACC/FTIR-like measurement made since the late 1950s. By a comparison to coincident TCCON (Total Carbon Column Observing Network) measurements, we empirically demonstrate the useful quality of this suggested NDACC XCO_2 product (empirically obtained scatter between TCCON and NDACC is about 4 ‰ for daily mean as well as monthly mean comparisons, and the bias is 25 ‰). Our XCO_2 model is a simple regression model fitted to CarbonTracker results and the Mauna Loa CO_2 in situ records. A comparison to TCCON data suggests an uncertainty of the model for monthly mean data of below 3 ‰. We apply the method to the NDACC/FTIR spectra that are used within the project MUSICA (multi-platform remote sensing of isotopologues for investigating the cycle of atmospheric water) and demonstrate that there is a good consistency for these globally representative set of spectra measured since 1996: the scatter between the modelled and measured XCO_2 on a yearly time scale is only 3 ‰.

1 Introduction

The Network for the Detection of Atmospheric Composition Change (NDACC – formerly called Network for the Detection of Stratospheric Change, NDSC) first started measurements of atmospheric components in 1991 (Kurylo, 1991). The network is composed of more than 70 high-quality, remote-sensing research stations. Initially, the main focus was on stratospheric species and on observing the long-term change of the ozone layer, subsequently, the tropospheric composition and its link to climate change also became an important topic. Within this network, the Infrared Working Group (IRWG) operates more than 20 ground-based Fourier transform infrared (FTIR) spectrometers spread worldwide that measure the absorption of direct sunlight by atmospheric gases in the middle infrared (MIR). The strength of the NDACC is the fact that it is a network that offers numer-

ous long time series of many species and at globally distributed sites. There are many studies dealing with the long-term records of several trace gases measured within this network, e.g. $ClONO_2$, HCl and HF (e.g. Rinsland et al., 2003; Kohlhepp et al., 2012), H_2O (Schneider et al., 2012), CH_4 (Sussmann et al., 2012; Sepúlveda et al., 2014), N_2O (Angelbratt et al., 2011a), CO and C_2H_6 (Angelbratt et al., 2011b) and O_3 (Vigouroux et al., 2008). These studies would strongly benefit from a tool that is able to prove the multi-year stability of instrument precision and accuracy, later on referred to as the long-term data consistency between the different sites throughout the network. Please note that in the following the NDACC/FTIR data sets are referred to as NDACC.

In this context, it is helpful to refer to TCCON (Total Carbon Column Observing Network), which is another network of ground-based FTIR spectrometers and closely affiliated to the Infrared Working Group of NDACC. The major difference between the TCCON and NDACC is that for the former, solar spectra in the near infrared (NIR) are recorded (Wunch et al., 2011). The first TCCON measurements were obtained in 2004. The TCCON NIR spectra cover O_2 absorption signatures. Since atmospheric O_2 concentrations are very stable and well-known, TCCON O_2 measurements can be used for demonstrating the consistency of the TCCON measurements throughout the network. The NDACC MIR spectra do not cover O_2 absorption signatures and at the moment, there is no direct way to assess the long-term consistency of the NDACC FTIR measurements in analogy to TCCON. Goldman et al. (2007) attempted to use N_2 for this purpose. Atmospheric N_2 concentrations are very stable, well-known, and there are absorption signatures in the MIR between 2400 and 2450 cm^{-1}, but due to spectroscopic issues sufficient accuracy could not be achieved.

In this paper, we propose using the total column dry-air mole fractions of CO_2 (XCO_2) as global proxy for reviewing the long-term consistency of the MIR measurements. CO_2 has well isolated and easily detectable absorption signatures in the MIR spectral region. However, in contrast to O_2 or N_2, CO_2 is variable with a continuing yearly increase as well as seasonal cycles with latitudinal variations, which must be accounted for in assessing the network-wide consistency. As an example, Fig. 1 shows different XCO_2 data sets for the Karlsruhe FTIR station. The seasonal cycle becomes clearly visible in the TCCON retrieval product (green triangles, TCCON), in the TCCON a priori (blue open diamonds, TCap), in the mid-infrared retrieval product using TCCON a priori (red dots, $NDACC_{TCap}$) and in the mid-infrared retrieval product using the fixed WACCM (The Whole Atmosphere Community Climate Model, http://waccm.acd.ucar.edu) a priori (black squares, NDACC; the fixed WACCM a priori is shown as orange open triangles). Please note, the here called NDACC XCO_2 products are obtained from the retrieval setup as suggested by us for this study. They are no standard NDACC/FTIR products and thus

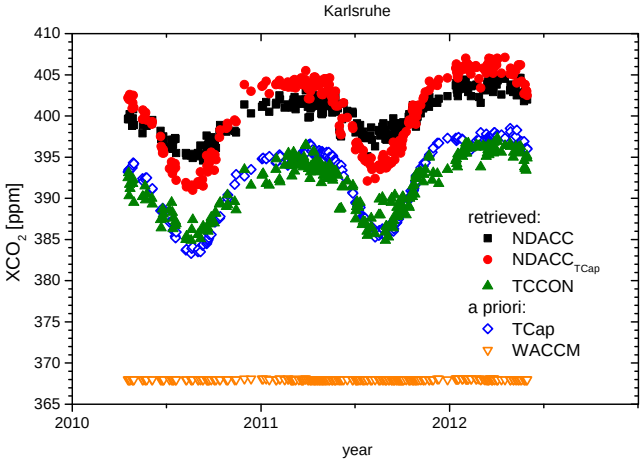

Figure 1. XCO_2 data sets for Karlsruhe, Germany (mid-latitude, Northern Hemisphere). Black: retrieved from NDACC spectra using fixed WACCM a priori, red: retrieved from NDACC spectra using TCCON a priori, green: TCCON, blue: TCCON a priori, orange: WACCM a priori.

not available via the NDACC database. The impact of the different a priori assumptions on the retrievals are discussed in detail in Sect. 2.2 and 4).

Schneider et al. (2012) showed that the de-seasonalised annual mean XCO_2 data obtained at 10 different NDACC/FTIR stations agree within a few per mill (when taking into account the 6 ‰ difference between the Southern and Northern Hemisphere), demonstrating that XCO_2 can be used as a reference for consistency for long-term measurements and for periods when many different NDACC/FTIR stations provide measurements. In this work, we further elaborate on the approach of Schneider et al. (2012). We want to check our data sets for shifts and biases caused by e.g. instrumental failure or change of instruments for the whole data sets of all used sites. Our objective is to design a method that allows an assessment of the network consistency of any NDACC/IRWG-like FTIR measurement even if it has been limited to a short campaign or to a period when the number of NDACC/FTIR stations was still relatively small (e.g. before the 2000s). For this purpose we present a simple XCO_2 retrieval method that can easily be adopted to any site where an NDACC-like measurement has been made since the 1950s. The measured XCO_2 data are then referenced to a multi-regression XCO_2 model that provides information on the long-term, seasonal, and latitudinal behaviour of XCO_2.

In the following section, we present our simple XCO_2 retrieval strategy for NDACC/FTIR spectral data and briefly discuss the main differences to the more complex TCCON XCO_2 retrieval setup. Section 3 contains a description of our XCO_2 model. We demonstrate the accuracy of the model by a comparison to TCCON data. In Sect. 4, we perform an empirical validation of our NDACC XCO_2 data, using coincident TCCON data as a reference. In Sect. 5, the XCO_2 model and

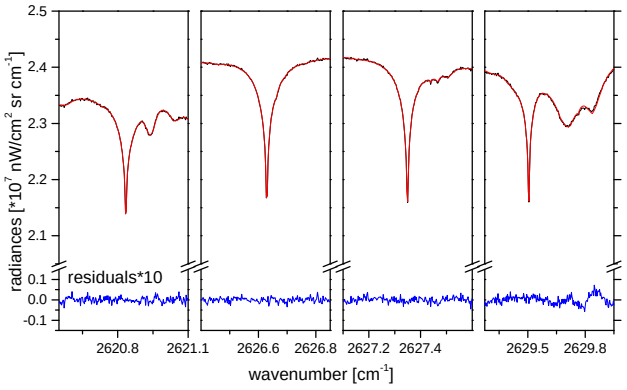

Figure 2. The four spectral microwindows used for the ground-based FTIR retrieval. Shown is an example of a typical measurement at Karlsruhe (04 June 2010, 07:36 UT, solar elevation 38.15°). (26 October 2010, 08:44 UT, solar elevation: 18.1°). Black: measured spectrum, red: simulation and residuals (difference between measurement and simulation) multiplied by a factor of 10 (blue).

the NDACC measurements are used for demonstrating the consistency of the observations made at 10 globally representative FTIR sites.

This study uses more than 17000 individual observations made since 1996 on more than 6000 days and during different periods recorded at 10 globally distributed NDACC/FTIR sites. These are the sites that are currently contributing to the MUSICA project (multi-platform remote sensing of isotopologues for investigating the cycle of atmospheric water, Schneider et al., 2012). The paper concludes with a summary and an outlook.

2 The XCO_2 NDACC retrieval

2.1 The CO_2 retrieval setup

The ground-based FTIR systems measure solar absorption spectra using high-resolution Fourier transform spectrometers. For our analysis we apply the retrieval code PROFFIT and the included radiative transfer code PROFFWD (Hase et al., 2004). PROFFIT has been used for many years in the ground-based FTIR community for evaluating high-resolution solar absorption spectra. Details about the retrieval principles are described by e.g. Schneider et al. (2012) or Sepúlveda et al. (2012).

The spectral microwindows that are used for this study are shown in Fig. 2 and Table 1 (Kohlhepp, 2007). In addition to CO_2 we have considered spectroscopic signatures of the interfering species H_2O and CH_4. The spectroscopic line parameters for CO_2 and CH_4 have been taken from the HITRAN (High-Resolution Transmission Molecular Absorption) 2008 database (Rothman et al., 2009), while for H_2O we applied the HITRAN 2009 update (www.cfa.harvard.edu/hitran/).

Table 1. Spectral microwindows chosen for the NDACC CO_2 retrieval shown in this study.

	Spectral microwindows (cm^{-1})
MW1	2620.550–2621.100
MW2	2626.400–2626.850
MW3	2627.100–2627.600
MW4	2629.275–2629.950

2.2 Profile scaling and a priori information

An important aspect of our study is that we use a rather simple retrieval setup (fixed a priori and simple scaling retrieval). This assures that the method can be correctly and consistently applied for different sites and time periods, without any risk of inconsistency due to a priori and constraints. The spectral windows, as depicted in Fig. 2, contain some weak H_2O, HDO and CH_4 lines. In order to minimise the spectral interferences due to the highly variable atmospheric amounts of H_2O and HDO, we investigated a two-step retrieval strategy. First, the H_2O profile is determined by the MUSICA H_2O retrieval (Schneider et al., 2010, 2012, 2015). As a second step, CO_2 is retrieved by simultaneous scaling with its interfering species CH_4 and H_2O. Here, the retrieved daily mean H_2O profile as a result of the first step is used as a priori information. However, we found that the H_2O and HDO absorptions are rather weak so that not applying the two-step strategy does not significantly affect the CO_2 results. For CO_2 and CH_4, we apply the climatological entries from WACCM version 6, provided by NCAR (National Center for Atmospheric Research, J. Hannigan, private communication, 2009). The WACCM a priori profile of CO_2 for Karlsruhe is the black line in Fig. 3. We use this single WACCM a priori profile for all the NDACC CO_2 retrievals made at Karlsruhe (Fig. 1). The WACCM simulations can vary between sites, but for each site a temporally constant a priori is applied. This is a main difference with respect to the TCCON retrieval setup, which is much more complex in this context. The CO_2 a priori information used by the TCCON retrieval for the actual TCCON data set varies from day to day, which has to be properly considered for comparisons with other data sets.

For the TCCON retrievals the CO_2 a priori information varies from day to day, which has to be properly considered if one wants to setup a TCCON-like XCO_2 retrieval. The coloured lines in Fig. 3 represent the TCCON a priori profiles for Karlsruhe for 4 days in 2011 during different seasons that are used to calculate the TCCON data set (Sect. 3.2.1).

The a priori assumptions affect the retrieval results. For sites where NDACC and TCCON measurements are made simultaneously, we made two different retrievals with the NDACC MIR spectra. First we applied our simple retrieval recipe (fixed WACCM a priori), and then we calculated the results when using the TCCON strategy (daily varying a pri-

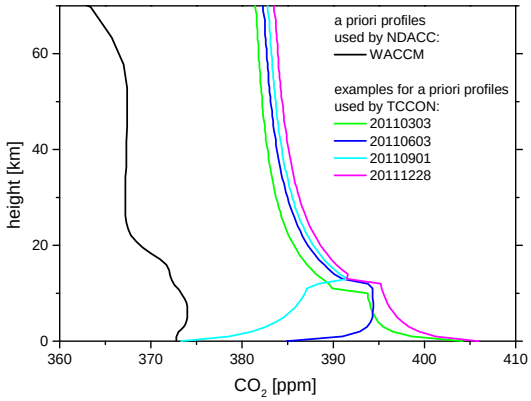

Figure 3. A priori profiles for Karlsruhe: WACCM v6 (used as a priori for NDACC retrieval) and some examples used as a priori for TCCON retrieval.

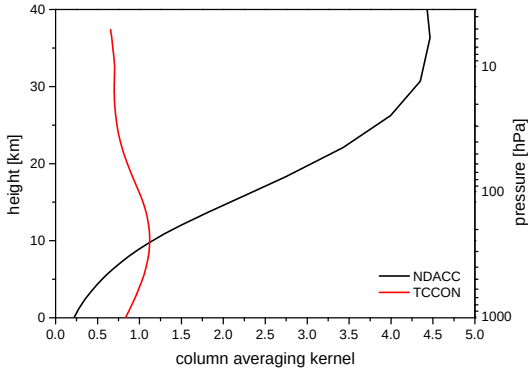

Figure 4. Column-averaging kernel for Karlsruhe (NDACC; 04 June 2010, 07:36 UT, solar elevation 38.15°) and Lamont (TCCON) for the same solar elevation.

ori). Figure 1 shows the different retrieval results for Karlsruhe. The NDACC XCO_2 values obtained with the fixed WACCM a priori and the varying TCCON a priori are depicted as the orange and red dots, respectively. In addition, the figure shows the TCCON XCO_2 product (green dots). The a priori XCO_2 assumptions are plotted as blue and orange dots (for the fixed WACCM and the varying TCCON assumptions, respectively). The influence of the a priori information on the series and especially on the seasonal cycle will be further discussed in Sect. 4. Typical column-averaging kernels for NDACC and TCCON which represent the height-dependent sensitivity of the retrieved total column to perturbations of the partial columns at the various atmospheric levels are shown in Fig. 4. A value of 4.5 at 30 km means, that an input disturbance at these altitude levels would be significantly overestimated, which is a consequence of the lower values at heights between ground and 5 km. However note that the variability in the stratosphere is very small. An ideal column-averaging kernel would be unitary (Connor et al., 2008). Compared to TCCON, the NDACC spectra have less sensitivity in the lower troposphere, which means that small variations in that region won't be captured in detail. However, in the following we will show that this is sufficient for our study as we are interested in variabilities on timescales longer than a month. On these timescales, the model we use (Sect. 3) is valid, so the difference between NDACC XCO_2 and the model can be used as proxy for the stability of the NDACC data.

NCEP (National Centers for Environmental Prediction) analysis data at 12 UT are used for daily temperature and pressure profiles for all sites (e.g. Lait, 2015).

Table 2. Uncertainty sources used for our error estimation. The second column gives the assumed uncertainty value and the third column the assumed partitioning between statistical and systematic sources.

Error source	Uncertainty	Stat./Syst.
Baseline (channelling/offset)	0.02 %/0.1 %	50/50
Instrumental line shape (Mod. eff./phase error)	1 %/0.01 rad	50/50
Temperature profile	2–5 K	70/30
Line of sight	0.1°	90/10
Solar lines (Intensity/ν-scale)	1 %/10^{-6}	80/20
Spectroscopic parameters (S/γ)	2/5 %	0/100

2.3 Error estimation

The assumptions we made for our error calculations are listed in Table 2. Apart from uncertainties in the spectroscopic parameters (line strength S and pressure broadening γ), which are purely systematic, we assume a systematic and a statistical contribution for each uncertainty. An exception is the error due to measurement noise, which we assume to be purely random.

The errors, estimated with the error calculation implemented in PROFFIT for a typical measurement at Karlsruhe station (04 June 2010, 07:36 UT, solar elevation 38.15°), are listed in Table 3. The systematic error is clearly dominated by spectroscopy, mainly due to the pressure broadening error. The leading random error source is the measurement noise followed by the baseline uncertainty.

2.4 Calculation of XCO_2

NDACC XCO_2 is calculated by dividing the CO_2 total column by the dry pressure column (DPC). The DPC is obtained by converting the ground pressure to column air concentra-

Table 3. Statistical and systematic errors in the Karlsruhe total CO_2-column due to the assumed uncertainty sources of Table 2. The total error represents the root-sum-squares of all errors.

Error	Statistical [%]	Systematic [%]
Measurement noise	0.20	
Baseline	0.17	0.17
Instrumental line shape	0.02	0.02
Temperature	0.10	0.07
Line of sight	0.04	0.01
Solar lines	0.02	0.01
Spectroscopy		4.22
TOTAL	0.33	4.23

tion (e.g. Deutscher et al., 2010):

$$\mathrm{DPC} = \frac{\mathrm{P_s}}{\mathrm{m_{dryair}} \cdot \mathrm{g}(\varphi)} - \frac{\mathrm{m_{H_2O}}}{\mathrm{m_{dryair}}} \cdot \mathrm{H_2O_{col}} \quad (1)$$

where P_s is the surface pressure in Pascals, m_{dryair} the molecular mass of the dry air ($\sim 28.96 \times 10^{-3}\,N_A$ kg molecule^{-1}), m_{H_2O} the molecular mass of the water vapour ($\sim 18 \times 10^{-3}\,N_A$ molecule^{-1}), H_2O_{col} the water vapour total column amount (in molecules m^{-2}, N_A Avogadro's constant ($\sim 6.022 \times 10^{23}$ molecules mol^{-1}) and $g(\varphi)$ the latitude-dependent surface acceleration due to gravity. H_2O_{col} is a result of the MUSICA retrieval (Schneider et al., 2010, 2012) and surface pressure is taken from NCEP.

This method is not expected to be as precise as the TCCON method which uses the measured O_2 column as reference when calculating the dry pressure column. However, it has the advantage that it can be easily applied to all historic measurements made in the 2600–3000 cm^{-1} spectral region (both H_2O and CO_2 can be retrieved in the same filter region so there is no need for additional coinciding measurements).

3 The XCO_2 model

3.1 Description of the model

As reference for the XCO_2 measurements we use an empirical XCO_2 model. The empirical model formula includes a polynomial fit with an empirical lookup adjustment to the Mauna Loa series (http://co2now.org/Current-CO2/CO2-Now/scripps-co2-data-mauna-loa-observatory.html) (Keeling et al., 2001, 2005), considering global trace gas distribution given by CarbonTracker (http://www.esrl.noaa.gov/gmd/ccgg/carbontracker/) (Peters et al., 2007). The formula is a modification of that used in Reuter et al. (2012), suggested by F. Hase (private communication, 2012), allowing the calculation of reasonable values with an improved latitude-dependency also outside the fit period.

The only inputs required for the model in addition to the Mauna Loa time series and CarbonTracker are the time, latitude and typical surface pressure of the measurement site. The XCO_2 is modelled via

$$y(t, l_r, P_{\mathrm{stat}}) = c_0 + d_{\mathrm{NDACC}} \cdot d_{\mathrm{h}} \cdot \mathrm{ML_a}$$
$$(a_{2\pi} \sin(2\pi t + \phi_{2\pi}) + a_{4\pi} \sin(4.0\pi t + \phi_{4\pi})), \quad (2)$$

where t is the decimal year, l_r the latitude in rad and P_{stat} the typical pressure at the measurement site. c_0 contains the time- and latitude-dependent CO_2-increase:

$$c_0 = (\mathrm{ML_{smooth}} + \mathrm{ML_{corr}})\,(e_1 + e_2),$$

where ML_{smooth} describes the inter-annual increase of CO_2:

$$\mathrm{ML_{smooth}} = 316.5 + 0.8407\,t_\mathrm{d} + 0.012\,t_\mathrm{d}^2,$$

with $t_d = t - 1960$. ML_{corr} are yearly correction factors that consider the year-to-year variations of the Mauna Loa series, compared to a polynomial fit. All ML_{corr} values are listed in Appendix C (Table C1). The coefficients e_1 and e_2 construct latitudinal gradients on the predicted long-term CO_2 concentration:

$$e_1 = a_1 + \frac{a_2}{\exp^{2.5\,(l_\mathrm{r}+0.2)} + 1.0}$$
$$e_2 = \frac{a_3}{\exp^{-6.0\,(l_\mathrm{r}-0.9)} + 1.0}$$

with $a_1 = 1.0018$, $a_2 = -0.0106576$ and $a_3 = -2.132\exp^{-3}$. The amplitude of the Mauna Loa series is described by

$$\mathrm{ML_a} = 0.5\,(3.0 + 0.006\,(t - 1959.0)).$$

As in Reuter et al. (2012), the seasonal cycle has a 12- and a 6-month period with a latitudinal-dependent phase:

$$a_{2\pi} = 0.8\left(0.2 + \frac{4.0}{\exp^{-3.5\,(l_\mathrm{r}-0.5)} + 1.0}\right)$$
$$a_{4\pi} = 0.5\left(0.05 + \frac{1.7}{\exp^{-3.5\,(l_\mathrm{r}-0.5)} + 1.0}\right)$$
$$\phi_{2\pi} = -2.75 + \frac{3.3}{\exp^{-2.8\,(l_\mathrm{r}+0.2)} + 1.0}$$
$$\phi_{4\pi} = 1.45 + 1.9\sin(1.4\,l_\mathrm{r}).$$

To consider the influence of the measurement height on the seasonal cycle, we implemented the damping factor d_h:

$$d_\mathrm{h} = \frac{(P_\mathrm{stat} - P_\mathrm{TP})}{(P_\mathrm{grnd} - P_\mathrm{TP})}, \quad (3)$$

where P_{TP} is the typical tropopause pressure for the site latitude and P_{grnd}=1013.25 hPa.

For approximating the actual atmospheric XCO_2 values, d_{NDACC} is set to unity. For reproducing NDACC-type CO_2 observations, it is a smaller value than unity (accounting for the non-ideal column sensitivity of the retrieval; for details see Sect. 4.2).

Table 4. Overview of collaborating ground-based NDACC/TCCON FTIR stations.

Site	Country	Latitude	Longitude	Height [m a.s.l.]	Institution
Eureka (NDACC + TCCON)	Canada	80.1° N	86.4° W	610	U. Toronto
Ålesund (NDACC + TCCON)	Norway	78.9° N	11.9° E	21	U. Bremen/AWI
Kiruna (NDACC)	Sweden	67.8° N	20.4° E	419	KIT IMK-ASF/IRF
Sodankylä (TCCON)	Finland	67.4° N	26.6° E	188	FMI ARC
Bremen (NDACC + TCCON)	Germany	53.1° N	8.9° E	27	U. Bremen
Karlsruhe (TCCON + MIR)	Germany	49.1° N	8.4° E	110	KIT IMK-ASF
Jungfraujoch (NDACC)	Switzerland	46.6° N	8.0° E	3580	U. Liège
Izaña (NDACC + TCCON)	Spain	28.3° N	16.5° W	2367	KIT IMK-ASF/AEMET
Wollongong (NDACC + TCCON)	Australia	34.5° S	150.9° E	30	U. Wollongong
Lauder (NDACC + TCCON)	New Zealand	45.1° S	169.7° E	370	NIWA
Arrival Heights (NDACC)	Antarctica	77.8° S	166.7° E	250	NIWA

Due to the fact that the model does not include meteorological fields, the calculated values can only be valid on a monthly time scale and not on a synoptic or daily time scale. To account for that, we only compare monthly mean data, which are calculated from daily means and we require that the standard error of the so calculated monthly mean is smaller than 5 ‰.

3.2 Empirical uncertainty assessment of the model

As in Reuter et al. (2012), we use the TCCON data set for validating our model. In the following, we briefly introduce TCCON and discuss the quality of the TCCON XCO_2 data, after that we compare our model calculation to the TCCON reference.

3.2.1 The TCCON XCO_2 data set

TCCON is a network of ground-based Fourier transform spectrometers that record direct solar spectra in the NIR. It was founded in 2004 and operates around 20 spectrometers spread worldwide. From these spectra, accurate and precise column-averaged abundances of atmospheric constituents including CO_2, CH_4, N_2O, HF, CO, H_2O and HDO, are retrieved.

To retrieve trace gas columns from the measured spectra, the software package GGG2012, developed by G. Toon (JPL), is used (Wunch et al., 2011, 2012). For CO_2 a profile scaling retrieval approach is applied. As interfering species, HDO, H_2O and CH_4 are considered. There are two selected windows: the central wave numbers are 6220.0 and 6339.5 cm^{-1} with spectral widths of 80 and 85 cm^{-1}, respectively. The spectroscopic data of Toth et al. (2008) and Rothman et al. (2009) with empirical extensions of G. Toon (personal communication, 2014) are used.

TCCON uses time-dependent CO_2 a priori profiles. Up to 10 km, the a priori profile is the result of an empirical model, based on fits to GLOBALVIEW data and independent vertical profiles (e.g. AirCore, aircraft overflights). In the stratosphere, an age-dependent profile is assumed. Examples of TCCON a priori profiles for different seasons are shown in Fig. 3. Already this empirical a priori model provides a good estimator for the actual atmospheric XCO_2 and the difference between the a priori model and the TCCON result is often smaller than 1 % (typical scatter between blue and green symbols in Fig. 1). The objective of TCCON is to significantly improve the estimations of the model and get an accuracy for XCO_2 of better then 2 ‰. Such high and network-wide precision is considered mandatory for using XCO_2 for carbon cycle research (Olsen and Randerson, 2004).

TCCON data products are column-averaged dry-air mole fractions, which for e.g. XCO_2 are calculated as (Wunch et al., 2011):

$$XCO_2 = 0.2095 \frac{CO_2^{col}}{O_2^{col}} . \quad (4)$$

Taking the ratio to the co-observed O_2 column has the advantage that correlated errors of CO_2 and O_2 are reduced. The time-dependent TCCON a priori assumptions cause a pronounced annual cycle and inter-annual trend in the TCCON XCO_2 a priori data (blue dots in Fig. 1).

There have been several calibration campaigns (Washenfelder et al., 2006; Deutscher et al., 2010; Wunch et al., 2010, 2012; Messerschmidt et al., 2011) that all consistently yield a calibration factor of 0.989 ± 0.001 for XCO_2. The data we use in this study have all been corrected by this calibration factor.

TCCON data sets (GGG2012) have been downloaded from the TCCON database (http://tccon.ipac.caltech.edu/). Due to the fact that some of these measurements have been recorded with faulty laser sampling boards (Messerschmidt et al., 2010), they were biased relative to the data recorded after the board exchange. Dohe et al. (2013) have developed a re-sampling algorithm that has been either already applied to most of the affected data before the upload or the effect was negligible (TCCON, 2013). Of the data sets used, only the time series of Bremen and Wollongong had to be manu-

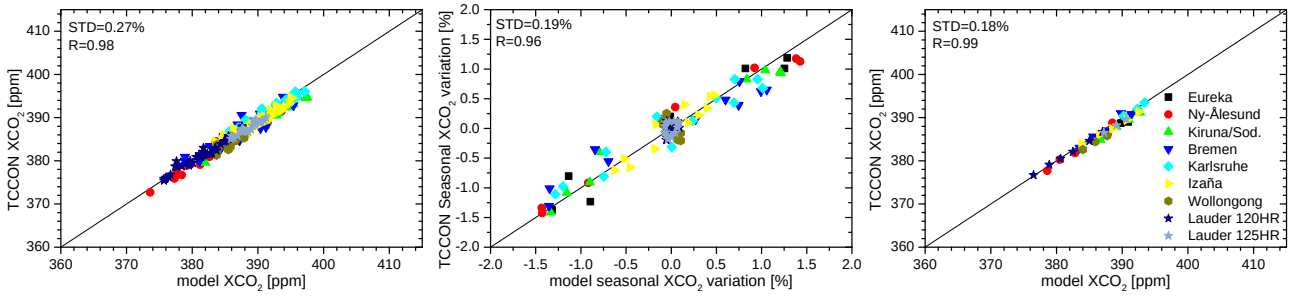

Figure 5. Correlation of TCCON vs. XCO_2 model for the time period 2005–2012. Left: monthly means, middle: detrended seasonal cycles, right: de-seasonalised yearly means. Added is the one-to-one correlation (black line). At Lauder, two TCCON instruments have been used (Bruker 120HR/125HR).

ally corrected before our comparisons. In the case of Bremen, all measurements made before 18 June 2009 needed a correction of -1.2 ppm; the Wollongong data measured until 22 July 2011 have been shifted by -1.0 ± 1 ppm. A detailed description of this error can be found on the TCCON web site (TCCON, 2013) as well as in Dohe et al. (2013) and Messerschmidt et al. (2010).

3.2.2 Comparison of modelled XCO_2 and TCCON XCO_2

The TCCON sites have been chosen to fit to our actual set of NDACC sites (Table 4). At Eureka, Ny-Ålesund, Bremen, Karlsruhe, Izaña, Wollongong and Lauder NDACC and TCCON measurements are performed at the same site. At Kiruna, Jungfraujoch and Arrival Heights there are no TCCON measurements. However, Kiruna is located close to the TCCON station of Sodankylä (67.3668° N, 26.631° E, 0.188 m a.s.l.), which is 260 km east and around 40 km south of Kiruna. Therefore, the Sodankylä TCCON data is paired with the Kiruna NDACC and the modelled XCO_2 data.

Figure 5 shows the correlation of TCCON versus the modelled XCO_2 data set for the time period 2005–2012 for all the TCCON sites we work with in this study. The left graph shows the correlation for monthly mean data, which is the time scale that can be reproduced by the model (please recall that it cannot capture synoptic time scale variations). The correlation coefficient is $R = 0.98$ and the scatter (SD of the difference between model and measurement) is 2.7 ‰. We investigate this agreement in more detail by looking at different time scales: the seasonal cycle (or intra-annual time scale) and the long-term evolution (or inter-annual time scale).

The middle graph of Fig. 5 compares the measured and modelled detrended seasonal cycles calculated for each site. It is expressed in percentage values because it is the seasonal variation with respect to the de-seasonalised data. For its calculation we first remove the inter-annual trend and then calculate the mean for each month of the year (the inter-annual trend is removed by fitting a Fourier series according to e.g. Gardiner et al., 2008). We observe that the model captures well the variation on this seasonal time scale ($R = 0.96$ and a scatter of 1.9 ‰). Detailed documentation of the seasonal cycles for the different sites can be found in Appendix A (Fig. A1).

The correlation of the de-seasonalised yearly means is plotted in the right graph (it is the yearly mean as calculated from the data after removing the seasonal cycle). On this inter-annual time scale the agreement is very good ($R = 0.99$ and a scatter of 1.8 ‰).

Overall, the model and measurements agree very well. According to the scatter between the model and the TCCON data, the model is able to predict the XCO_2 amounts on a monthly time scale with a precision of better than 3 ‰ and on a yearly time scale with a precision of better than 2 ‰.

4 Empirical validation of the NDACC XCO_2 data

In this section, we want to check the quality of the NDACC XCO_2 data. As for the validation of the model (see previous Section), we use the TCCON XCO_2 data set as reference to check the quality and the influence of the retrieval strategy on the data set. When comparing TCCON and our XCO_2 product, we have to be aware that the retrieval strategies are different: while for our NDACC retrieval we use a fixed a priori for each site, for TCCON the a priori is changing from day-to-day. The empirical validation is made for the eight sites of our study, where TCCON and NDACC measurements are made at the same site (or nearby, as in Kiruna/Sodankylä) and on the same day (we use daily mean data as the basis for the comparison).

In the following, we present two types of comparison. First, we generate an XCO_2 product from NDACC measurements that uses the same varying a priori information as the TCCON retrieval, hereinafter called $NDACC_{TCap}$. Both the TCCON and the $NDACC_{TCap}$ XCO_2 data sets are influenced by the same a priori information. This means that differences between these two data sets are rather directly linked to the different measurements (different spectral resolution

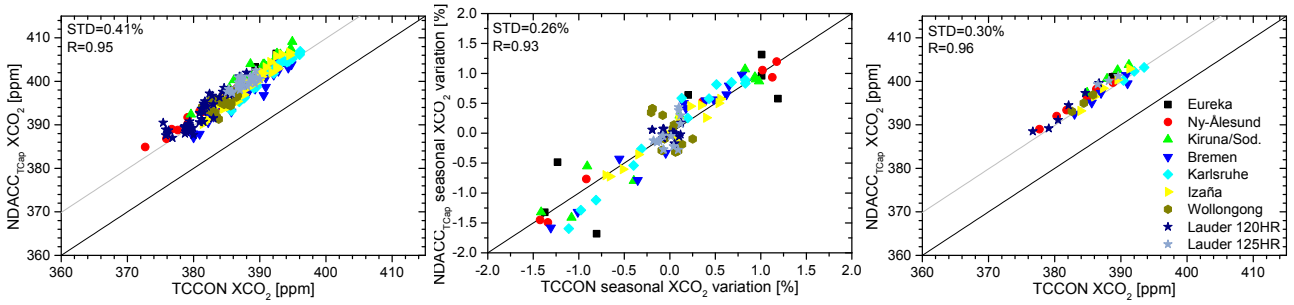

Figure 6. As Fig. 5 but for NDACC XCO_2 applying the varying TCCON a priori (NDACC$_{TCap}$) vs. TCCON. The black line represents the one-to-one correlation, the grey line is the correlation shifted by 2.5 %.

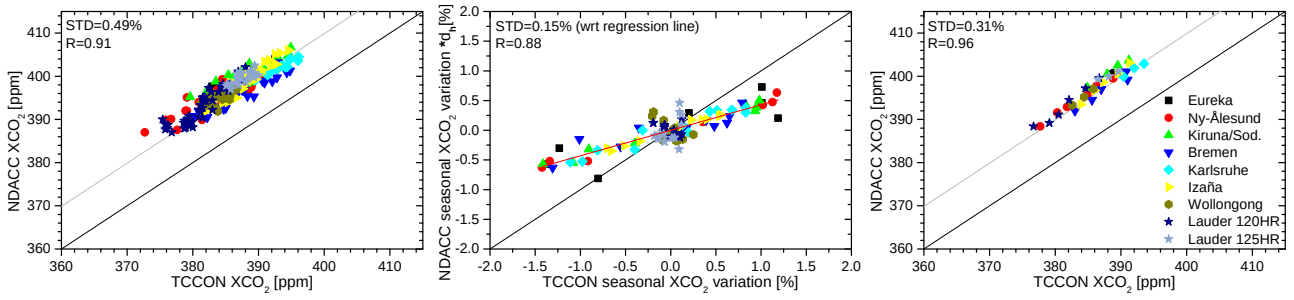

Figure 7. As Fig. 5 but for NDACC XCO_2 applying the fixed WACCM a priori. Left: monthly means, middle: detrended seasonal cycles with regression line (red), given standard deviation with respect to the regression line, right: de-seasonalised yearly means. The black line represents the one-to-one correlation, the grey line is the correlation shifted by 2.5 %.

and spectral region). Second, we compare the XCO_2 NDACC product (obtained by the fixed a priori) with the TCCON product (varying a priori). Differences in these two data sets are due to the different measurements and the different a priori assumptions. However, since the TCCON product is of a well known and high absolute quality, this second comparison exercise can reveal the actual capability of the XCO_2 NDACC retrieval when using a fixed a priori (recall that the advantage of this recipe is that it can be easily adopted for any site and any time period).

4.1 Comparison of NDACC and TCCON XCO_2 when using the same varying a priori

Figure 6 shows the comparison between the NDACC$_{TCap}$ and the TCCON XCO_2 data sets. The panels from the left to the right are analogous to Fig. 5 for the different time scales: left panel for monthly mean data, central panel for detrended intra-annual monthly mean variations and right panel for deseasonalised yearly means.

We observe a good correlation between the two data sets. The scatter is about 4 ‰ on a monthly time scale and 3 ‰ on a yearly time scale. However, there is a significant systematic difference. The NDACC XCO_2 values are by 25 ‰ larger than the TCCON XCO_2 values. There are two reasons that might explain the systematic difference. First, our NDACC XCO_2 product is calculated using DPC (Eq. 1) whereas for TCCON O_2 is used (Eq. 4). However, the O_2 columns are known to be 2 % too high (Wunch et al., 2010) and applying the O_2 columns instead of the DPC values for the calculation of the NDACC XCO_2 data would yield about 2 % smaller values and thus a much smaller difference with respect to the TCCON XCO_2 data. Note that the TCCON calibration is made for XCO_2 not for CO_2. Second, NDACC and TCCON measure in different spectral regions, thus part of the differences are probably caused by inconsistencies between the spectroscopic data (Sects. 2.1 and 3.2.1).

The comparison of the seasonal variations (central panel) also reveals good agreement. When using the same a priori as TCCON, the NDACC measurements can reproduce the TCCON seasonal variation within 2.6 ‰ (scatter between the two data sets). A detailed overview on the seasonal cycles for the different sites is given in the Appendix A (Fig. A1).

The main interest of this study are monthly or longer time scales, which are decisive for the reliability of trend analyses. These time scales can be well captured by the model (Sect. 3). However, often TCCON and NDACC measurements are made on the same day, and we can compare the measurements on a daily time scale. Although it is not of direct interest for our long-term study, the day-to-day NDACC vs. TCCON comparison can serve as a good measure for the quality of the NDACC XCO_2 product. We found that the day-to-day scatter between the NDACC and TCCON data

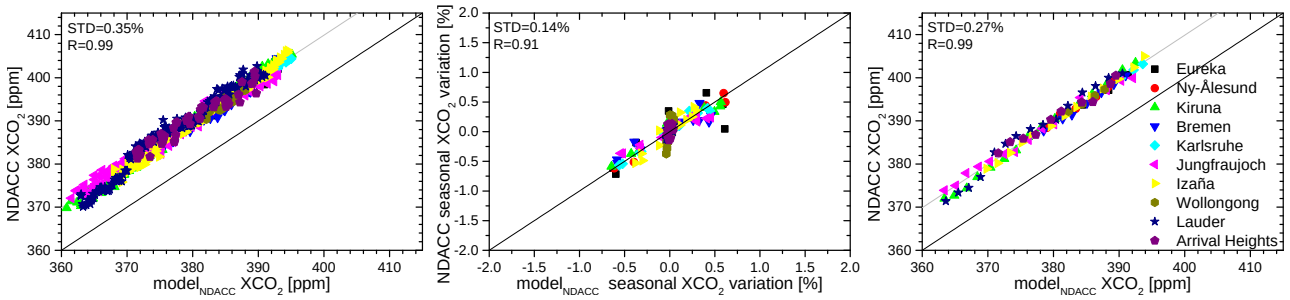

Figure 8. As Fig. 5 but for NDACC XCO_2 applying the WACCM fixed a priori and model$_{NDACC}$ and for the time period 1996–2012.

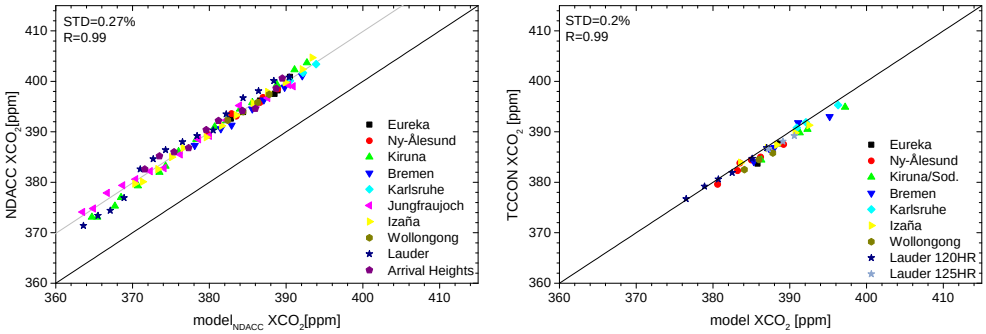

Figure 9. Correlations of the yearly means. Left: NDACC vs. model NDACC (1996–2012), right: TCCON vs. model (2005–2012).

sets is generally within 4 ‰ (Appendix B). This good agreement nicely documents that the CO_2 signatures recorded by the NDACC spectra can serve as a reliable quality proxy for the NDACC data sets. For some sites the agreement with TCCON is even within 3 ‰. In addition, Fig. B1 shows that the NDACC XCO_2 data can reveal the deficits of the simple XCO_2 a priori model in a similar manner as the TCCON XCO_2 data. This suggests that the NDACC XCO_2 data might even be useful for carbon cycle research. For this purpose a precision for XCO_2 of at least 2 ‰ is required (Olsen and Randerson, 2004). This high precision can be achieved by the TCCON measurements and the results of Appendix B suggest that for some stations an NDACC product can achieve a similar high precision. A further investigation of a possible extension of the TCCON XCO_2 time series by NDACC XCO_2 data is beyond the scope of our paper and currently under investigation by M. Buschmann (University of Bremen, private communication, 2014).

4.2 Comparison of NDACC (fixed a priori) and TCCON XCO_2 (varying a priori)

Figure 7 shows the same as Fig. 5, but for NDACC XCO_2 obtained when using a fixed a priori. For the comparison of de-seasonalised yearly means (right panel), we observe a very good correlation ($R = 0.96$), a rather small scatter of 3.1 ‰ and a systematic difference of 25 ‰. This is almost identical to what we observe in Fig. 6 for the comparison between the $NDACC_{TCap}$ and the TCCON XCO_2 data sets. The NDACC retrieval that uses a fixed a priori is sufficient to retrieve the long-term evolution of XCO_2. It is not necessary to use an a priori that simulates this long-term behaviour. For the monthly mean data (left panel, Fig. 7), the correlation is poorer than observed in the left panel of Fig. 6. As explained in the following, this poorer agreement is mainly due to the failure of the NDACC XCO_2 data to capture the full amplitude of the seasonal cycle.

On seasonal time series, variations in the CO_2 profile occur mostly in the lower to middle troposphere, meaning that the variation occurs in the shape of the profile. Such profile shape variations cannot be captured well by the NDACC retrieval, which simply scales a climatological mean profile (WACCM profile), thus leading to a damped seasonality of the time series due to the reduced column sensitivity in the lower troposphere (Fig. 4). Since the seasonal variation is limited to the troposphere, the damping factor depends on the tropopause pressure relative to the site's surface pressure. We assume the damping factor due to the fixed a priori as

$$d_{\mathrm{NDACC}} \sim \frac{1}{d_{\mathrm{h}}}. \quad (5)$$

Here, d_{h} is calculated according to Eq. (3).

The central panel of Fig. 7 plots the relative seasonal variation of the NDACC data multiplied by d_{h} versus the relative seasonal variations of the TCCON data. We get a good linear correlation ($R = 0.88$) and a linear regression line with

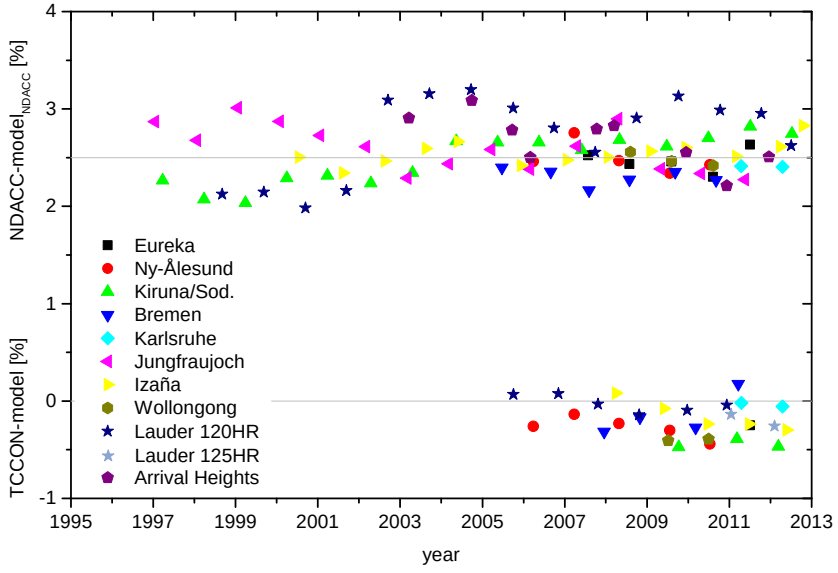

Figure 10. Time series of the differences of the yearly means between measurement and respective model. Top: NDACC-model$_{NDACC}$, bottom: TCCON-model.

a slope of 0.43. This indicates that a single damping factor $d_{NDACC} = 0.43 \times \frac{1}{d_h}$ is sufficient for describing the damped seasonal variations at all NDACC/FTIR sites. A detailed overview on the damped seasonal cycles for the different sites is given in the Appendix (Fig. A2). Note: d_h cancels out in Eq. 2 and $d_{NDACC} \times d_h$ becomes a constant factor.

5 XCO_2 as global proxy for long-term consistency

In this section, we check the NDACC/FTIR time series for long-term consistency by comparing the NDACC XCO_2 measurements with the XCO_2 model calculations.

5.1 Comparison of modelled XCO_2 and NDACC XCO_2

The reduced seasonality due to the fixed a priori used for the NDACC retrievals must be taken into account; i.e. we apply the damping factor $d_{NDACC} = 0.43 \cdot \frac{1}{d_h}$ for our model calculations according to Eq. (2) (hereinafter, we call these model calculations with damped seasonality model$_{NDACC}$). Figure 8 shows the same as Fig. 5, but for the correlation between the NDACC XCO_2 and the model$_{NDACC}$ data for the time period 1996–2012. NDACC measurements started many years before the TCCON measurements and there are many more data points in Fig. 8 than in Fig. 5. Nevertheless, the correlation to the model is almost as good for NDACC as for TCCON. For monthly mean data (left panel of Fig. 8) we get a correlation coefficient R of 0.99 and a scatter of 3.5 ‰. For the de-seasonalised yearly mean data (right panel), the scatter is even as small as 2.7 ‰. In agreement with the NDACC vs. TCCON comparison, we observe a systematic positive bias in the NDACC XCO_2 data of about 25 ‰. The damped seasonality of the NDACC time series is well captured by the model$_{NDACC}$ data (central panel of Fig. 8). This documents that the model can also evaluate the NDACC data consistency on intra-annual time scales.

As the subset of NDACC/FTIR sites we are using within this study is representative of nearly all latitudes (Table 4), we conclude that the model$_{NDACC}$ is valid for assessing the consistency of all NDACC/FTIR measurements made around the globe.

5.2 Network-wide long-term stability

Finally, to document the network-wide long-term stability, we compare annual means, not to be mistaken for the de-seasonalised annual means shown in the comparisons Fig. 5 to Fig. 8. Figure 9 compares the measurements and their respective model with NDACC vs. model$_{NDACC}$ on the left and TCCON vs. model on the right. Figure 10 shows the same data, but plotted as a function of time. All these comparisons show that the agreement between measurement and respective model is excellent. There's no drift in the differences, which might be expected when using one fixed a priori over several years. Long-term and station-to-station variabilities of the measurements with respect to the model are within 1 % for both the NDACC and TCCON data sets. The scatter is within 3 ‰ for NDACC-model$_{NDACC}$ and 2 ‰ for TCCON-model.

6 Conclusions

Mid-infrared high resolution solar absorption spectra have been recorded for many years and at many sites around the globe. Most of these activities are organised within the NDACC and have a high potential for investigating the long-term change of our atmosphere on a global scale. However, such investigations require data that are very consistent throughout many years and between the different sites.

In this work, we present a method that allows an assessment of the consistency of any mid-infrared high-resolution solar absorption measurement (2600–3000 cm^{-1} spectral region) made since the late 1950s. The method uses the difference between XCO_2 retrieved from the spectra and as simulated by a model. Both the retrieval and the model are designed in a way that allows their easy adoption to any measurement site.

The XCO_2 retrieval uses a fixed CO_2 a priori profile (obtained from WACCM simulations), which is scaled during the retrieval process. Furthermore, we use NCEP temperature and pressure profiles. This simple scaling retrieval setup using a time-independent a priori allows it to be easily adopted for any site around the globe and for any mid-infrared high-resolution solar absorption measurement if reliable data for the surface pressure and analysis temperature profiles are available. The XCO_2 model is driven by Mauna Loa data (long-term evolution) and CarbonTracker results (latitudinal gradients) and should thus capture well the period covered by the Mauna Loa CO_2 record, which starts in the 1950s.

We use the TCCON XCO_2 data to empirically demonstrate the good quality of the NDACC XCO_2 product and of the XCO_2 model simulations. For the period where TCCON data are available, the scatter for monthly mean data between TCCON and model is 2.7 ‰ and between TCCON and NDACC it is 4.1 ‰ (when using the same a priori). We identify a clear systematic difference between the TCCON and NDACC data of 25 ‰ (our NDACC product overestimates the calibrated TCCON values), which is very likely due to an error in the MIR spectroscopic CO_2 parameters. Identifying this clear bias is a side aspect of our study. The important metric we are interested in is the stability of the difference. Furthermore, we demonstrate that using a fixed a priori instead of a daily varying a priori almost exclusively affects the amplitude of the seasonal variations. We show that the respective damping of the seasonal amplitude can be described by a consistent parametrisation for all the different sites and can be very easily considered in the model simulations.

We apply the developed method to the NDACC/FTIR spectra that have so far been contributing to the project MUSICA. These spectra have been measured since 1996 at 10 stations that are distributed around the globe. We found a scatter between the yearly mean NDACC data and the model of about 3 ‰. This provides strong evidence for the very good long-term data consistency between these NDACC/FTIR sites and is a good reliability and consistency test for the long-term trends of tropospheric species measured at these sites.

Appendix A: Seasonal cycles as determined from the different data sets

All seasonal cycles determined from the different data sets are plotted in Fig. A1. For better comparability, only the subset of measurements is considered, with both, NDACC and TCCON measurements at the same day. Black represents the NDACC values, calculated with fixed a priori information, red are the NDACC values, when the TCCON a priori information is used, green is the seasonal variation of the TCCON time series and blue are the modelled values. It is obvious that the fixed a priori information (black symbols) leads to a reduced sensitivity for the seasonal cycle.

To consider this, the damping factor d_{NDACC} is implemented (Sect. 4). The comparison of the detrended seasonal cycle of the whole NDACC data set (black) with the damped model version (red) is shown in Fig. A2. Both are in very good agreement.

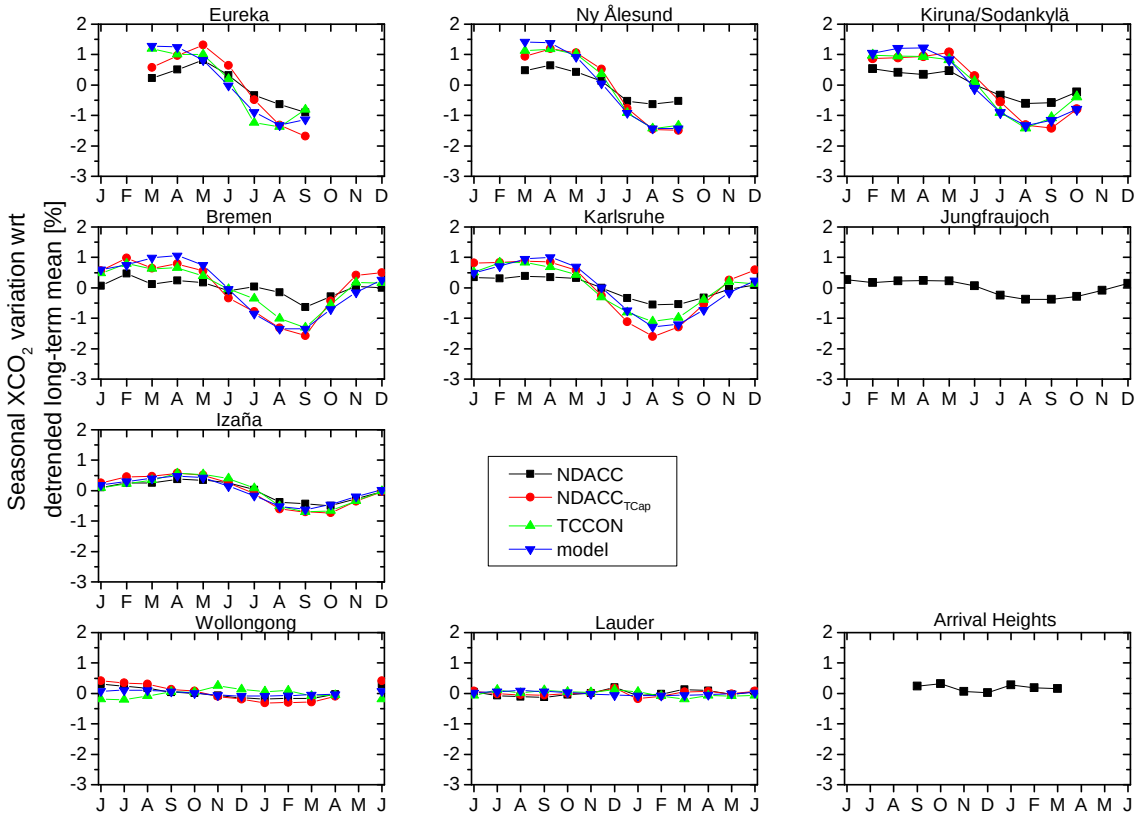

Figure A1. Seasonal cycles. Black: NDACC with fixed WACCM a priori, red: NDACC with same a priori as TCCON, green: TCCON and blue: model.

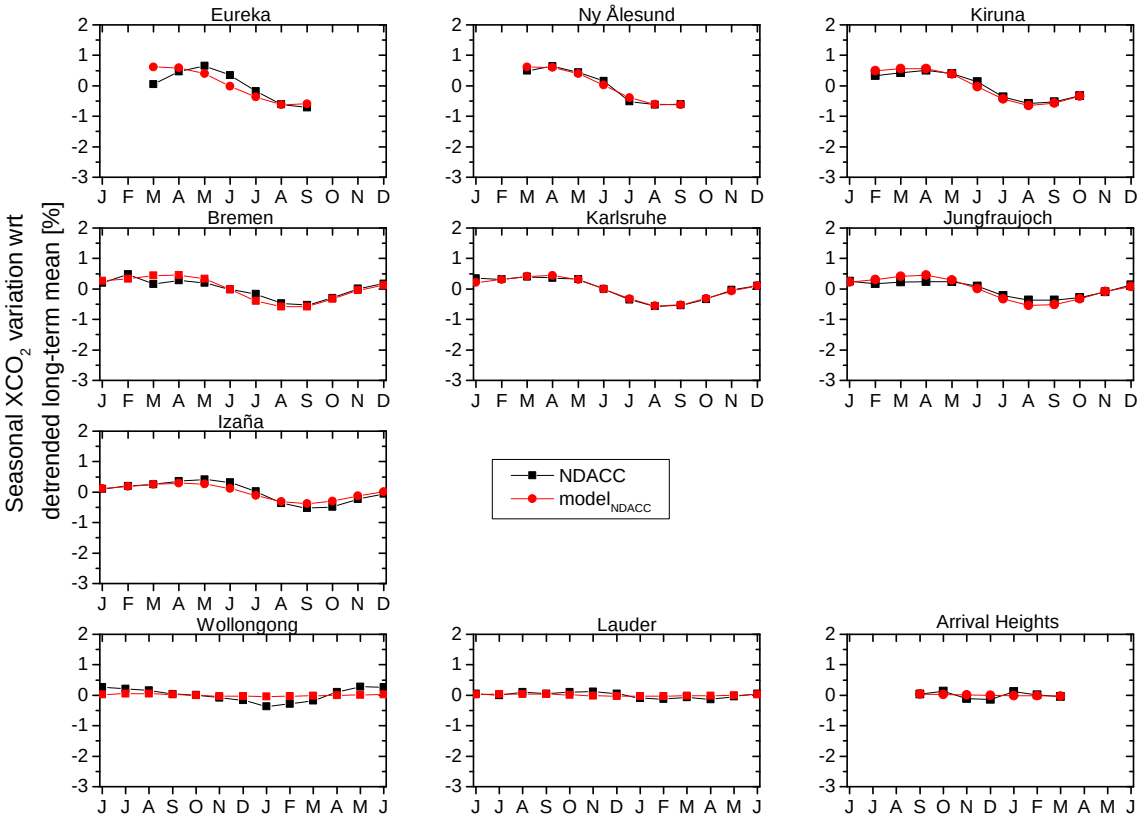

Figure A2. As Fig. A1, but now only NDACC and the damped model ($model_{NDACC}$) are compared.

Appendix B: Comparison of day-to-day XCO_2 variations between TCCON and NDACC

Depicted in Fig. B1 is the correlation of the difference between NDACC (with TCCON a priori, $NDACC_{TCap}$) and TCCON a priori vs. the difference between TCCON and TCCON a priori. Plotted are the daily means with the number of considered days N, correlation coefficient R, mean relative difference (MRD) and standard deviation (SD). The black line is the one-to-one correlation shifted by 2.5 %. By subtracting the a priori, we compare in this plot directly the information that comes from the measurements and compare the capabilities of NDACC and TCCON in improving the XCO_2 estimations as provided by the TCCON a priori model. In the case of Lauder, two TCCON instruments have been used (Bruker 120HR: black points, 125HR: grey points).

There is a higher correlation for northern sites, where there is more variability (R between 0.5 and 0.7). The scatter values (SD) are between 3 to 5 ‰. As mentioned before (Sects. 4 and 5), there's a clear systematic difference between the two data. Besides the systematic difference, the agreement of both data sets is good and demonstrates that in the MIR XCO_2 can be obtained at a very good quality (the NDACC measurements improve the empirical TCCON a priori model in a similar way as the TCCON measurements).

We would like to note that the consistency of NDACC and TCCON XCO_2 products might even be further improved by using the same retrieval software and consistent line parameters. The here compared NDACC product works with the TCCON a priori model, but for the retrievals we use the PROFFIT software and the HITRAN spectroscopy (instead of the GGG software with empirical extensions of G. Toon (personal communication, 2014) for the spectroscopy used for the TCCON retrieval).

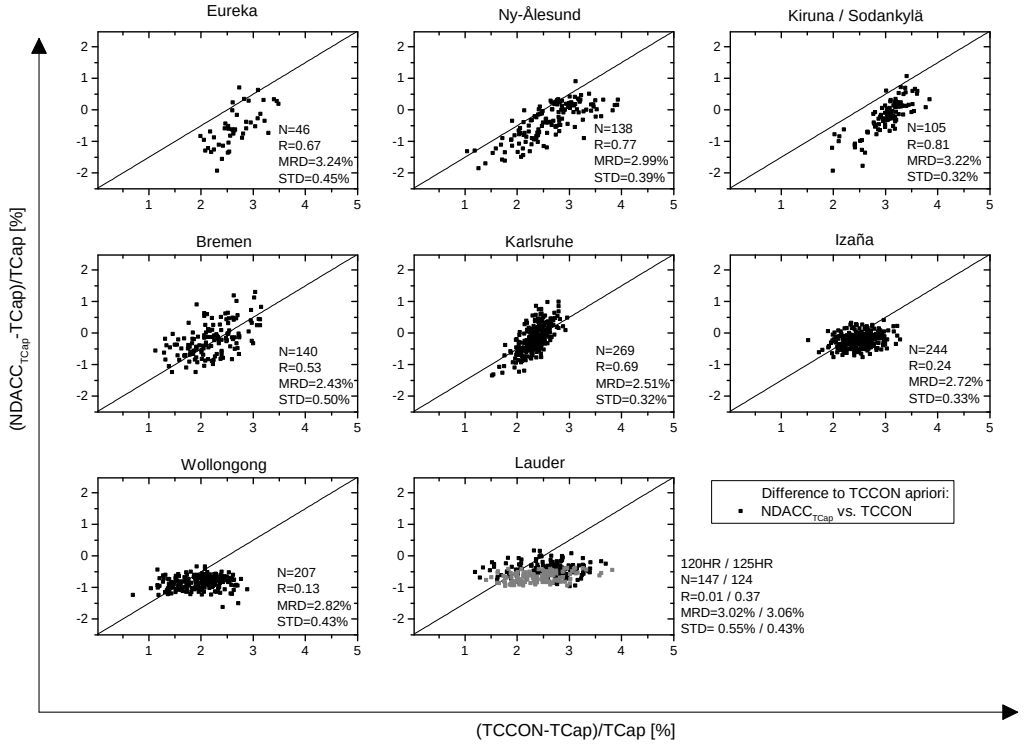

Figure B1. Correlation between (NDACC$_{TCap}$-TCap) and (TCCON-TCap). The black line represents the one-to-one correlation shifted by 2.5 %. The grey squares in the Lauder graph represent the data measured with the 125HR instrument, whereas the black squares are the data measured with the 120HR instrument.

Appendix C: List of ML_{corr} values

Listed in Table C1 are all yearly correction factors used in our XCO_2 model (Sect. 3). The correction factors $ML_{corr}(i)$ express the year-to-year variation between the Mauna Loa series compared to a polynomial fit, where i is the respective year. For all other years, $ML_{corr}(i)$ is set to 0. Values within 2 years are calculated by linear interpolation.

Table C1. Overview of all yearly correction factors used in our XCO_2 model (Sect. 3).

$ML_{corr}(1959) = 0.813$	$ML_{corr}(1973) = -0.405$	$ML_{corr}(1987) = 0.946$	$ML_{corr}(2001) = -0.624$
$ML_{corr}(1960) = 0.785$	$ML_{corr}(1974) = -0.509$	$ML_{corr}(1988) = 1.235$	$ML_{corr}(2002) = -0.546$
$ML_{corr}(1961) = 0.677$	$ML_{corr}(1975) = -0.666$	$ML_{corr}(1989) = 1.331$	$ML_{corr}(2003) = -0.303$
$ML_{corr}(1962) = 0.490$	$ML_{corr}(1976) = -0.768$	$ML_{corr}(1990) = 1.141$	$ML_{corr}(2004) = -0.098$
$ML_{corr}(1963) = 0.180$	$ML_{corr}(1977) = -0.633$	$ML_{corr}(1991) = 0.653$	$ML_{corr}(2005) = 0.074$
$ML_{corr}(1964) = -0.119$	$ML_{corr}(1978) = -0.376$	$ML_{corr}(1992) = 0.056$	$ML_{corr}(2006) = 0.134$
$ML_{corr}(1965) = -0.380$	$ML_{corr}(1979) = -0.104$	$ML_{corr}(1993) = -0.442$	$ML_{corr}(2007) = 0.097$
$ML_{corr}(1966) = -0.508$	$ML_{corr}(1980) = 0.138$	$ML_{corr}(1994) = -0.651$	$ML_{corr}(2008) = 0.016$
$ML_{corr}(1967) = -0.566$	$ML_{corr}(1981) = 0.294$	$ML_{corr}(1995) = -0.703$	$ML_{corr}(2009) = -0.061$
$ML_{corr}(1968) = -0.538$	$ML_{corr}(1982) = 0.403$	$ML_{corr}(1996) = -0.619$	$ML_{corr}(2010) = -0.053$
$ML_{corr}(1969) = -0.503$	$ML_{corr}(1983) = 0.481$	$ML_{corr}(1997) = -0.535$	$ML_{corr}(2011) = -0.073$
$ML_{corr}(1970) = -0.537$	$ML_{corr}(1984) = 0.537$	$ML_{corr}(1998) = -0.373$	$ML_{corr}(2012) = -0.064$
$ML_{corr}(1971) = -0.542$	$ML_{corr}(1985) = 0.580$	$ML_{corr}(1999) = -0.386$	
$ML_{corr}(1972) = -0.506$	$ML_{corr}(1986) = 0.702$	$ML_{corr}(2000) = -0.518$	

Acknowledgements. We would like to thank the many different technicians, PhD students, post-docs and scientists from the different research groups what have been involved in the NDACC-FTIR activities during the last two decades. Thanks to their excellent work (maintenance, calibration, observation activities, etc.), high-quality long-term data sets can be generated.

The Eureka measurements were made at the Polar Environment Atmospheric Research Laboratory (PEARL) by the Canadian Network for the Detection of Atmospheric Change (CANDAC), led by James R. Drummond and in part by the Canadian Arctic ACE Validation Campaigns, led by Kaley A. Walker. They were supported by the AIF/NSRIT, CFI, CFCAS, CSA, EC, GOC-IPY, NSERC, NSTP, OIT, PCSP and ORF. The authors wish to thank Rebecca Batchelor, Rodica Lindenmaier, PEARL site manager Pierre F. Fogal, the CANDAC operators and the staff at Environment Canada's Eureka weather station for their contributions to data acquisition and logistical and on-site support.

We thank the Alfred Wegener Institut Bremerhaven for support in using the AWIPEV research base, Spitsbergen, Norway. The work has been supported by EU-Project NORS.

We would like to thank Peter Völger for technical support at IRF Kiruna.

The University of Liège contribution has been supported by the A3C PRODEX program (Belgian Science Policy Office, Brussels), by the GAW-CH program of MeteoSwiss (Zürich), by the F.R.S.-FNRS and the Fédération Wallonie-Bruxelles. We thank the International Foundation High Altitude Research Stations Jungfraujoch and Gornergrat (HFSJG, Bern) for supporting the facilities needed to perform the observations.

E. Sepúlveda enjoyed a pre-doctoral fellowship thanks to the Spanish Ministry of Education.

Measurements at Wollongong are supported by the Australian Research Council, grant DP110103118.

Measurements at Lauder and Arrival Heights are core funded through New Zealand's Ministry of Business, Innovation and Employment. We would like to thank Antarctica New Zealand and the Scott Base staff for providing logistical support for the NDACC-FTIR measurement program at Arrival Heights.

TCCON data were obtained from the TCCON Data Archive, operated by the California Institute of Technology from the website at http://tccon.ipac.caltech.edu/.

This study has been conducted in the framework of the project MUSICA, which is funded by the European Research Council under the European Community's Seventh Framework Programme (FP7/2007–2013)/ERC Grant agreement number 256961.

We acknowledge the support by the Deutsche Forschungsgemeinschaft and the Open Access Publishing Fund of the Karlsruhe Institute of Technology.

The service charges for this open-access publication have been covered by a Research Centre of the Helmholtz Association.

Edited by: H. Worden

References

Angelbratt, J., Mellqvist, J., Blumenstock, T., Borsdorff, T., Brohede, S., Duchatelet, P., Forster, F., Hase, F., Mahieu, E., Murtagh, D., Petersen, A. K., Schneider, M., Sussmann, R., and Urban, J.: A new method to detect long term trends of methane (CH_4) and nitrous oxide (N_2O) total columns measured within the NDACC ground-based high resolution solar FTIR network, Atmos. Chem. Phys., 11, 6167–6183, doi:10.5194/acp-11-6167-2011, 2011a.

Angelbratt, J., Mellqvist, J., Simpson, D., Jonson, J. E., Blumenstock, T., Borsdorff, T., Duchatelet, P., Forster, F., Hase, F., Mahieu, E., De Mazière, M., Notholt, J., Petersen, A. K., Raffalski, U., Servais, C., Sussmann, R., Warneke, T., and Vigouroux, C.: Carbon monoxide (CO) and ethane (C_2H_6) trends from ground-based solar FTIR measurements at six European stations, comparison and sensitivity analysis with the EMEP model, Atmos. Chem. Phys., 11, 9253–9269, doi:10.5194/acp-11-9253-2011, 2011b.

Connor, B. J., Boesch, H., Toon, G., Sen, B., Miller, C., and Crisp, D.: Orbiting Carbon Observatory: Inverse method and prospective error analysis, J. Geophys. Res.-Atmos., 113, D05305, doi:10.1029/2006JD008336, 2008.

Deutscher, N. M., Griffith, D. W. T., Bryant, G. W., Wennberg, P. O., Toon, G. C., Washenfelder, R. A., Keppel-Aleks, G., Wunch, D., Yavin, Y., Allen, N. T., Blavier, J.-F., Jiménez, R., Daube, B. C., Bright, A. V., Matross, D. M., Wofsy, S. C., and Park, S.: Total column CO_2 measurements at Darwin, Australia – site description and calibration against in situ aircraft profiles, Atmos. Meas. Tech., 3, 947–958, doi:10.5194/amt-3-947-2010, 2010.

Dohe, S., Sherlock, V., Hase, F., Gisi, M., Robinson, J., Sepúlveda, E., Schneider, M., and Blumenstock, T.: A method to correct sampling ghosts in historic near-infrared Fourier transform spectrometer (FTS) measurements, Atmos. Meas. Tech., 6, 1981–1992, doi:10.5194/amt-6-1981-2013, 2013.

Gardiner, T., Forbes, A., de Mazière, M., Vigouroux, C., Mahieu, E., Demoulin, P., Velazco, V., Notholt, J., Blumenstock, T., Hase, F., Kramer, I., Sussmann, R., Stremme, W., Mellqvist, J., Strandberg, A., Ellingsen, K., and Gauss, M.: Trend analysis of greenhouse gases over Europe measured by a network of ground-based remote FTIR instruments, Atmos. Chem. Phys., 8, 6719–6727, doi:10.5194/acp-8-6719-2008, 2008.

Goldman, A., Tipping, R., Ma, Q., Boone, C., Bernath, P., Demoulin, P., Hase, F., Schneider, M., Hannigan, J., Coffey, M., and Rinsland, C.: On the line parameters for the $X^1\,\Sigma_g^+$ (1–0) infrared quadrupolar transitions of $^{14}N_2$, J. Quant. Spectrosc. Ra., 103, 168 – 174, doi:10.1016/j.jqsrt.2006.05.010, 2007.

Hase, F., Hannigan, J., Coffey, M., Goldman, A., Höpfner, M., Jones, N., Rinsland, C., and Wood, S.: Intercomparison of retrieval codes used for the analysis of high-resolution, ground-based FTIR measurements, J. Quant. Spectrosc. Ra., 87, 25–52., doi:10.1016/j.jqsrt.2003.12.008, 2004.

Keeling, C. D., Piper, S. C., Bacastow, R. B., Wahlen, M., Whorf, T. P., Heimann, M., and Meijer, H. A.: Exchanges of Atmospheric CO_2 and $^{13}CO_2$ with the Terrestrial Biosphere and Oceans from 1978 to 2000, I. Global aspects, SIO Reference Series, No. 01–06, Scripps Institution of Oceanography, San Diego, 88 pp., 2001.

Keeling, C. D., Piper, S. C., Bacastow, R. B., Wahlen, M., Whorf, T. P., Heimann, M., and Meijer, H. A.: A History of Atmospheric CO_2 and its effects on Plants, Animals, and Ecosystems, chap. Atmospheric CO_2 and $^{13}CO_2$ exchange with the terrestrial biosphere and oceans from 1978 to 2000: observations and carbon cycle implications., 83–113 pp., Springer Verlag, New York, 2005.

Kohlhepp, R.: Trend von CO_2 aus bodengebundenen FTIR Messungen in Kiruna, Seminararbeit am Institut für Meteorologie und Klimaforschung an der Universität Karlsruhe (TH), 36 pp., 2007.

Kohlhepp, R., Ruhnke, R., Chipperfield, M. P., De Mazière, M., Notholt, J., Barthlott, S., Batchelor, R. L., Blatherwick, R. D., Blumenstock, Th., Coffey, M. T., Demoulin, P., Fast, H., Feng, W., Goldman, A., Griffith, D. W. T., Hamann, K., Hannigan, J. W., Hase, F., Jones, N. B., Kagawa, A., Kaiser, I., Kasai, Y., Kirner, O., Kouker, W., Lindenmaier, R., Mahieu, E., Mittermeier, R. L., Monge-Sanz, B., Morino, I., Murata, I., Nakajima, H., Palm, M., Paton-Walsh, C., Raffalski, U., Reddmann, Th., Rettinger, M., Rinsland, C. P., Rozanov, E., Schneider, M., Senten, C., Servais, C., Sinnhuber, B.-M., Smale, D., Strong, K., Sussmann, R., Taylor, J. R., Vanhaelewyn, G., Warneke, T., Whaley, C., Wiehle, M., and Wood, S. W.: Observed and simulated time evolution of HCl, $ClONO_2$, and HF total column abundances, Atmos. Chem. Phys., 12, 3527–3556, doi:10.5194/acp-12-3527-2012, 2012.

Kurylo, M. J.: Network for the detection of stratospheric change, Proc. SPIE 1491, P. Soc. Photo-Opt. Ins., 168 (September 1, 1991), doi:10.1117/12.46658, 1991.

Lait, L. R.: Using the Goddard Automailer, available at: http://acd-ext.gsfc.nasa.gov/Data_services/ (last access: 12 January 2015), 2015.

Messerschmidt, J., Macatangay, R., Notholt, J., Petri, C., Warneke, T., and Weinzierl, C.: Side by side measurements of CO_2 by ground-based Fourier transform spectrometry (FTS), Tellus B, 62, 749–758, doi:10.1111/j.1600-0889.2010.00491.x, 2010.

Messerschmidt, J., Geibel, M. C., Blumenstock, T., Chen, H., Deutscher, N. M., Engel, A., Feist, D. G., Gerbig, C., Gisi, M., Hase, F., Katrynski, K., Kolle, O., Lavrič(, J. V., Notholt, J., Palm, M., Ramonet, M., Rettinger, M., Schmidt, M., Sussmann, R., Toon, G. C., Truong, F., Warneke, T., Wennberg, P. O., Wunch, D., and Xueref-Remy, I.: Calibration of TCCON column-averaged CO_2: the first aircraft campaign over European TCCON sites, Atmos. Chem. Phys., 11, 10765–10777, doi:10.5194/acp-11-10765-2011, 2011.

Olsen, S. C. and Randerson, J. T.: Differences between surface and column atmospheric CO_2 and implications for carbon cycle research, J. Geophys. Res.-Atmos., 109, 1–2, doi:10.1029/2003JD003968, 2004.

Peters, W., Jacobson, A. R., Sweeney, C., Andrews, A. E., Conway, T. J., Masarie, K., Miller, J. B., Bruhwiler, L. M. P., Pétron, G., Hirsch, A. I., Worthy, D. E. J., van der Werf, G. R., Randerson, J. T., Wennberg, P. O., Krol, M. C., and Tans, P. P.: An atmospheric perspective on North American carbon dioxide exchange: CarbonTracker, P. Natl. Acad. Sci., 104, 18925–18930, doi:10.1073/pnas.0708986104, 2007.

Reuter, M., Buchwitz, M., Schneising, O., Hase, F., Heymann, J., Guerlet, S., Cogan, A. J., Bovensmann, H., and Burrows, J. P.: A simple empirical model estimating atmospheric CO_2 background concentrations, Atmos. Meas. Tech., 5, 1349–1357, doi:10.5194/amt-5-1349-2012, 2012.

Rinsland, C. P., Mahieu, E., Zander, R., Jones, N. B., Chipperfield, M. P., Goldman, A., Anderson, J., Russell, J. M., Demoulin, P., Notholt, J., Toon, G. C., Blavier, J.-F., Sen, B., Sussmann, R., Wood, S. W., Meier, A., Griffith, D. W. T., Chiou, L. S., Murcray, F. J., Stephen, T. M., Hase, F., Mikuteit, S., Schulz, A., and Blumenstock, T.: Long-term trends of inorganic chlorine from ground-based infrared solar spectra: Past increases and evidence for stabilization, J. Geophys. Res.-Atmos., 108, D8, 4202, doi:10.1029/2002JD003001, 2003.

Rothman, L., Gordon, I., Barbe, A., Benner, D., Bernath, P., Birk, M., Boudon, V., Brown, L., Campargue, A., Champion, J.-P., Chance, K., Coudert, L., Dana, V., Devi, V., Fally, S., Flaud, J.-M., Gamache, R., Goldman, A., Jacquemart, D., Kleiner, I., Lacome, N., Lafferty, W., Mandin, J.-Y., Massie, S., Mikhailenko, S., Miller, C., Moazzen-Ahmadi, N., Naumenko, O., Nikitin, A., Orphal, J., Perevalov, V., Perrin, A., Predoi-Cross, A., Rinsland, C., Rotger, M., Šimečková, M., Smith, M., Sung, K., Tashkun, S., Tennyson, J., Toth, R., Vandaele, A., and Auwera, J. V.: The HITRAN 2008 molecular spectroscopic database, J. Quant. Spectrosc. Ra., 110, 533–572, doi:10.1016/j.jqsrt.2009.02.013, 2009.

Schneider, M., Toon, G. C., Blavier, J.-F., Hase, F., and Leblanc, T.: H_2O and δD profiles remotely-sensed from ground in different spectral infrared regions, Atmos. Meas. Tech., 3, 1599–1613, doi:10.5194/amt-3-1599-2010, 2010.

Schneider, M., Barthlott, S., Hase, F., Gonzâlez, Y., Yoshimura, K., García, O. E., Sepúlveda, E., Gomez-Pelaez, A., Gisi, M., Kohlhepp, R., Dohe, S., Blumenstock, T., Wiegele, A., Christner, E., Strong, K., Weaver, D., Palm, M., Deutscher, N. M., Warneke, T., Notholt, J., Lejeune, B., Demoulin, P., Jones, N., Griffith, D. W. T., Smale, D., and Robinson, J.: Ground-based remote sensing of tropospheric water vapour isotopologues within the project MUSICA, Atmos. Meas. Tech., 5, 3007–3027, doi:10.5194/amt-5-3007-2012, 2012.

Schneider, M., González, Y., Dyroff, C., Christner, E., Wiegele, A., Barthlott, S., García, O. E., Sepúlveda, E., Hase, F., Andrey, J., Blumenstock, T., Guirado, C., Ramos, R., and Rodríguez, S.: Empirical validation and proof of added value of MUSICA's tropospheric δD remote sensing products, Atmos. Meas. Tech., 8, 483–503, doi:10.5194/amt-8-483-2015, 2015.

Sepúlveda, E., Schneider, M., Hase, F., García, O. E., Gomez-Pelaez, A., Dohe, S., Blumenstock, T., and Guerra, J. C.: Long-term validation of tropospheric column-averaged CH_4 mole fractions obtained by mid-infrared ground-based FTIR spectrometry, Atmos. Meas. Tech., 5, 1425–1441, doi:10.5194/amt-5-1425-2012, 2012.

Sepúlveda, E., Schneider, M., Hase, F., Barthlott, S., Dubravica, D., García, O. E., Gomez-Pelaez, A., González, Y., Guerra, J. C., Gisi, M., Kohlhepp, R., Dohe, S., Blumenstock, T., Strong, K., Weaver, D., Palm, M., Sadeghi, A., Deutscher, N. M., Warneke, T., Notholt, J., Jones, N., Griffith, D. W. T., Smale, D., Brailsford, G. W., Robinson, J., Meinhardt, F., Steinbacher, M., Aalto, T., and Worthy, D.: Tropospheric CH4 signals as observed by

NDACC FTIR at globally distributed sites and comparison to GAW surface in situ measurements, Atmos. Meas. Tech., 7, 2337–2360, doi:10.5194/amt-7-2337-2014, 2014.

Sussmann, R., Forster, F., Rettinger, M., and Bousquet, P.: Renewed methane increase for five years (2007–2011) observed by solar FTIR spectrometry, Atmos. Chem. Phys., 12, 4885–4891, doi:10.5194/acp-12-4885-2012, 2012.

TCCON: Laser Sampling Errors, available at: https://tccon-wiki.caltech.edu/Network_Policy/Data_Use_Policy/Data_Description#Laser_Sampling_Errors (last access: 13 October 2014), 2013.

Toth, R., Brown, L., Miller, C., Malathy Devi, V., and Benner, D.: Spectroscopic database of CO_2 line parameters: 4300–7000 cm^{-1}, J. Quant. Spectrosc. Ra., 109, 906–921, doi:10.1016/j.jqsrt.2007.12.004, 2008.

Vigouroux, C., De Mazière, M., Demoulin, P., Servais, C., Hase, F., Blumenstock, T., Kramer, I., Schneider, M., Mellqvist, J., Strandberg, A., Velazco, V., Notholt, J., Sussmann, R., Stremme, W., Rockmann, A., Gardiner, T., Coleman, M., and Woods, P.: Evaluation of tropospheric and stratospheric ozone trends over Western Europe from ground-based FTIR network observations, Atmos. Chem. Phys., 8, 6865–6886, doi:10.5194/acp-8-6865-2008, 2008.

Washenfelder, R. A., Toon, G. C., Blavier, J.-F., Yang, Z., Allen, N. T., Wennberg, P. O., Vay, S. A., Matross, D. M., and Daube, B. C.: Carbon dioxide column abundances at the Wisconsin Tall Tower site, J. Geophys. Res.-Atmos., 111, D22305, doi:10.1029/2006JD007154, 2006.

Wunch, D., Toon, G. C., Wennberg, P. O., Wofsy, S. C., Stephens, B. B., Fischer, M. L., Uchino, O., Abshire, J. B., Bernath, P., Biraud, S. C., Blavier, J.-F. L., Boone, C., Bowman, K. P., Browell, E. V., Campos, T., Connor, B. J., Daube, B. C., Deutscher, N. M., Diao, M., Elkins, J. W., Gerbig, C., Gottlieb, E., Griffith, D. W. T., Hurst, D. F., Jiménez, R., Keppel-Aleks, G., Kort, E. A., Macatangay, R., Machida, T., Matsueda, H., Moore, F., Morino, I., Park, S., Robinson, J., Roehl, C. M., Sawa, Y., Sherlock, V., Sweeney, C., Tanaka, T., and Zondlo, M. A.: Calibration of the Total Carbon Column Observing Network using aircraft profile data, Atmos. Meas. Tech., 3, 1351–1362, doi:10.5194/amt-3-1351-2010, 2010.

Wunch, D., Toon, G. C., Blavier, J.-F. L., Washenfelder, R. A., Notholt, J., Connor, B. J., Griffith, D. W. T., Sherlock, V., and Wennberg, P. O.: The Total Carbon Column Observing Network, Philos. T. R. Soc. A, 369, 2087–2112, doi:10.1098/rsta.2010.0240, 2011.

Wunch, D., Wennberg, P., Toon, G., and the TCCON Science Team: TCCON Update – a comparison between GGG2009 and GGG2012, available at: https://tccon-wiki.caltech.edu/@api/deki/files/1534/=Wunch_TCCON_Update_20121008.pdf (last access: 11 March 2015), presented at the L2 Algorithms Meeting October 2–3, 2012.